Fluorescence polarization system for rapid COVID-19 diagnosis

Chang Yeol Lee[1#], Ismail Degani[2,3#], Jiyong Cheong[1,4], Jae-Hyun Lee[1,4], Hyun-Jung Choi[5], Jinwoo Cheon[1,4,6], Hakho Lee[1,2,4,7*]

[1] Institute for Basic Science (IBS), Center for Nanomedicine, Seoul, Korea
[2] Center for Systems Biology, Massachusetts General Hospital Research Institute, Boston, MA, USA
[3] Department of Electrical Engineering and Computer Science, Massachusetts Institute of Technology, Cambridge, MA USA
[4] Graduate Program of Nano Biomedical Engineering (NanoBME), Advanced Science Institute, Yonsei University, Seoul, Korea
[5] Department of Laboratory Medicine, Chonnam National University Medical School and Chonnam National University Hospital, Gwangju, Korea
[6] Department of Chemistry, Yonsei University, Seoul, Korea
[7] Department of Radiology, Massachusetts General Hospital, Harvard Medical School, Boston, MA, USA

[#]These authors contributed equally.

Corresponding Authors:
Hyun-Jung Choi, MD
Department of Laboratory Medicine
Chonnam National University Medical School and Chonnam National University Hospital
Gwangju, Korea
hyunjung.choi@chonnam.ac.kr

Jinwoo Cheon, PhD
Institute for Basic Science (IBS)
Center for Nanomedicine
Seoul, Korea
jcheon@yonsei.ac.kr

Hakho Lee, PhD
Center for Systems Biology
Massachusetts General Hospital
Boston, MA 02114, USA
hlee@mgh.harvard.edu

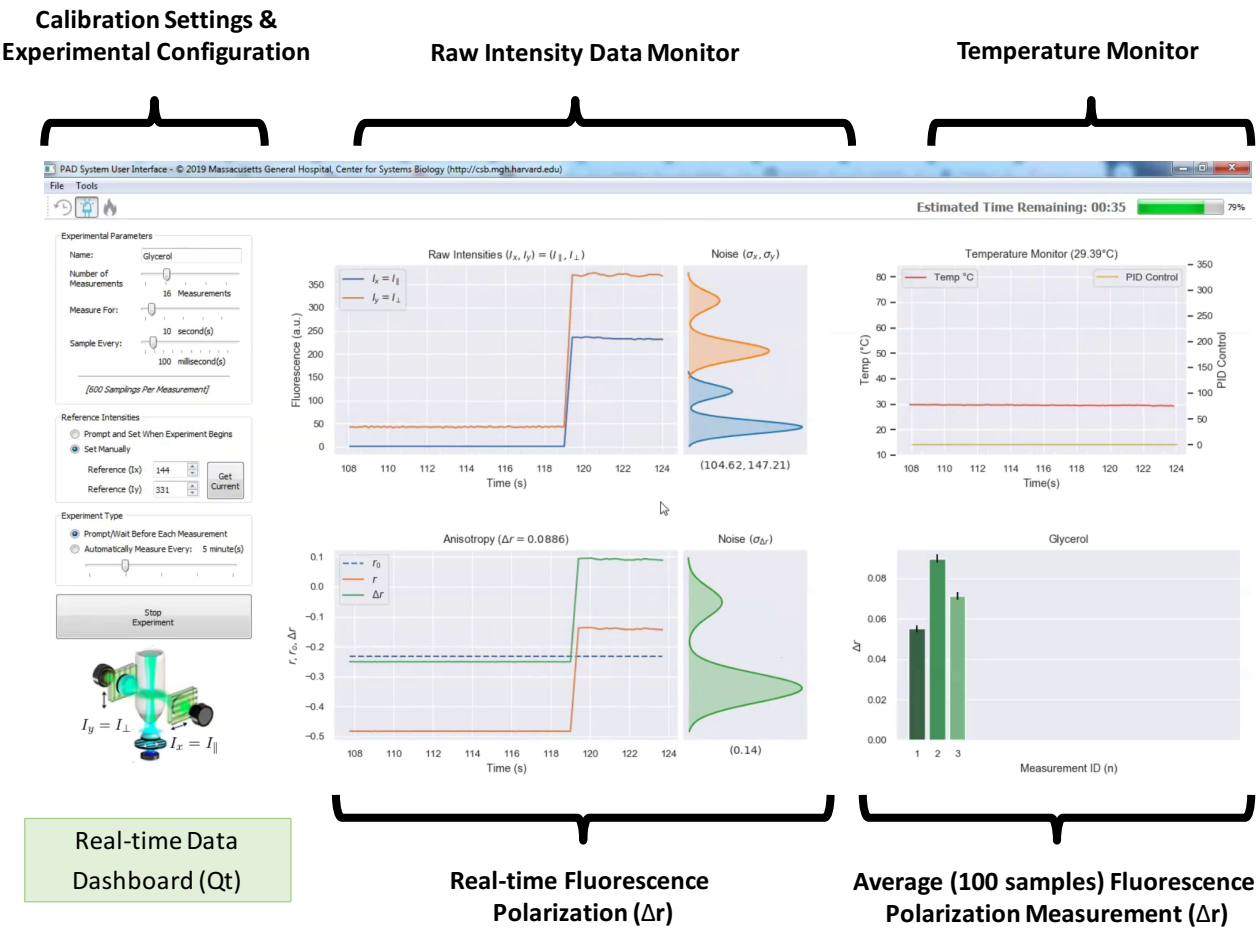

Fig. S1. Real-time user interface. At the far left is a configuration panel where experimental parameters can be tuned, including (i) the number of measurements to collect, (ii) how long each measurement should take, and (iii) how many samplings to average in order to obtain a reliable measurement. The reference fluorescence anisotropy (FA) value (r_0) can also be set here. The main dashboard is divided into four quadrants, where the user can monitor the raw fluorescent intensity for both parallel and perpendicular FA detectors (upper left), as well as a continuously computed FA value (lower left). Temperature and PID control signals are continuously monitored (upper right) and multiple patient samples can be analyzed sequentially in a batch and plotted (lower right). The dashboard is shown running on Windows 7-64 bit, though it is fully cross-platform and can run on a variety of operating systems that support the Qt GUI toolkit (MacOS/Linux).

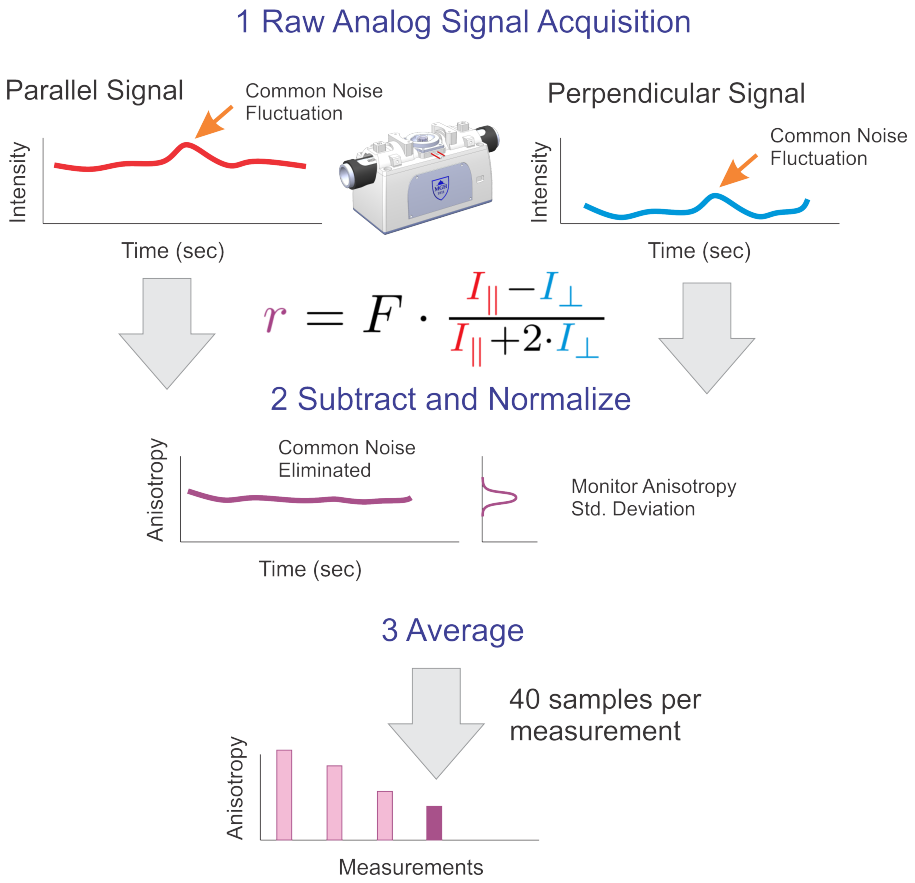

Fig. S2. CODA signal processing flow. In *step 1*, fluorescence intensity data from parallel (red) and perpendicular (blue) channels are captured as 14-bit integers every 0.1 sec. These signals may contain common noise (orange arrows). The channels are then subtracted, normalized, and scaled by factor *F*, leading to the continuous anisotropy plot of *step 2*. Note that the anisotropy measurement is free of the common noise fluctuations. A rolling standard deviation of the most recent 40 anisotropy samplings is monitored during data collection to ensure that the values are stable. Finally, in *step 3*, a measurement is taken as the average of 40 samples, provided that their standard deviation is less than 0.5%.

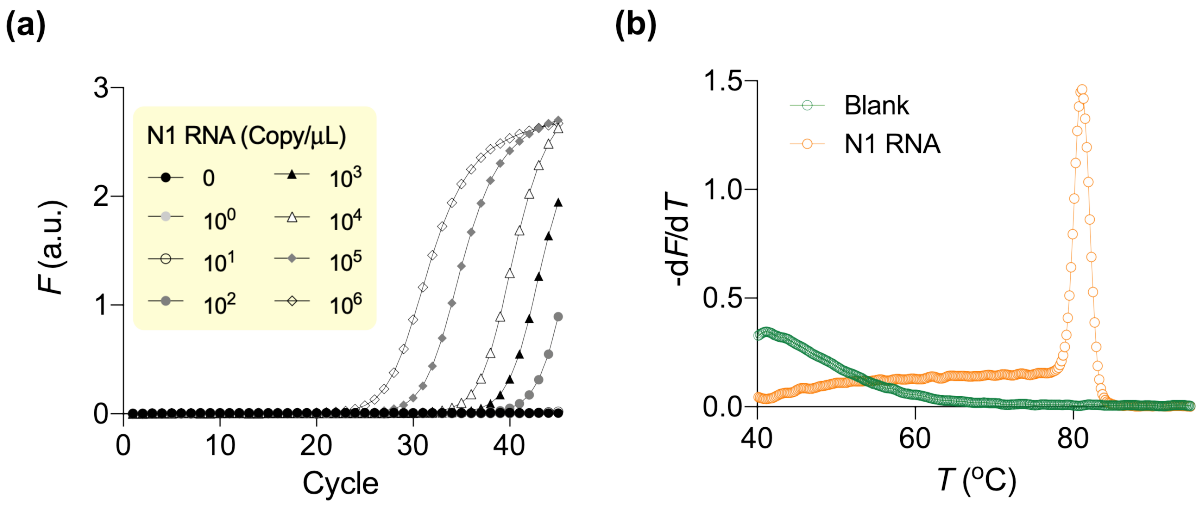

Fig. S3. qRT-PCR for N1 RNA. (a) Cycle-dependent fluorescent signals of qRT-PCR in the presence of serially diluted N1 RNA. **(b)** Melting curve analysis was carried out on RT-PCR product of N1 RNA to validate the results of qRT-PCR. The observed melting temperature (T_m = 81.1 °C) matches with a predicted value (80.6 °C).

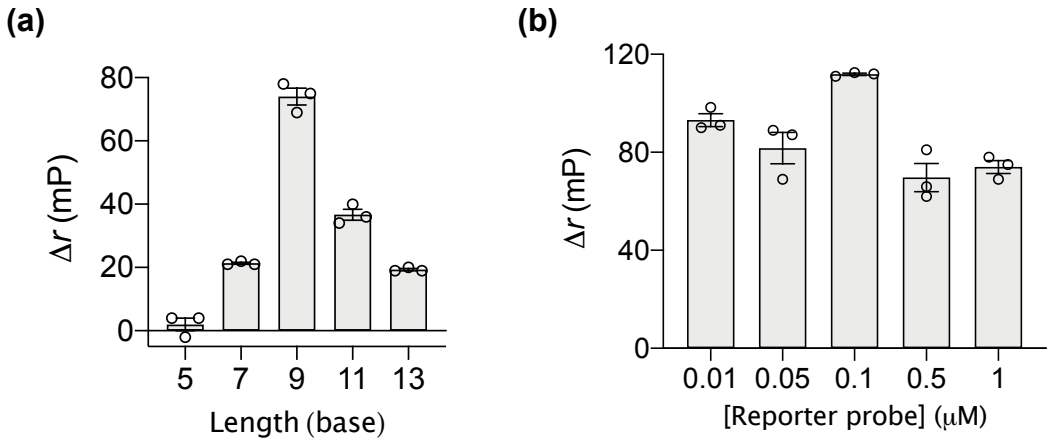

Fig. S4. Optimization of the reporter probe. (a) The length of the reporter probe was varied and the resulting anisotropy signal from CRISPR cleavage was measured. The optimal length was found to be 9 bases. **(b)** The concentration of the 9-base probe was optimized to achieve the maximal anisotropy signal. The optimal concentration was found to be 0.1 μM. The target concentration (SARS-CoV-2 plasmid control) was fixed at 10^3 copy/μL. All experiments were performed in triplicate and the data are displayed as means ± s.e.m.

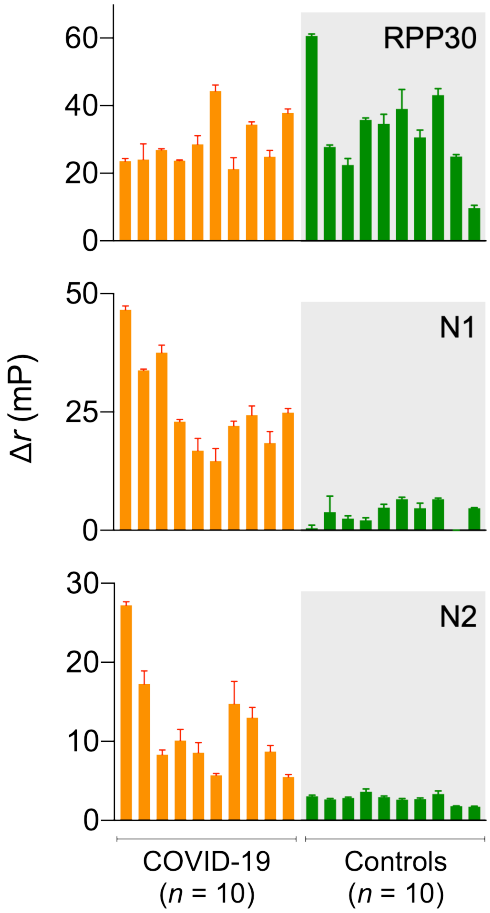

Fig. S5. CODA results of clinical samples. Three targets (N1, N2, RPP30) were assessed in clinical samples for COVID-19 detection. Data are displayed as mean ± s.e.m from triplicate measurements.

Table S1. Oligonucleotide sequences used in this study.

	Usage	Sequence (5' to 3')
CODA[a]	N1-Forward RPA primer	AGG CAG CAG TAG GGG AAC TTC TCC TGC TAG AAT
	N1-Reverse RPA primer	TTG GCC TTT ACC AGA CAT TTT GCT CTC AAG CTG
	N1-Forward Cas12a gRNA	UAA UUU CUA CUA AGU GUA GAU CAU CAC CGC CAU UGC CAG CC
	N1-Reverse Cas12a gRNA	UAA UUU CUA CUA AGU GUA GAU UUG CUG CUG CUU GAC AGA UU
	N2-Forward RPA primer	GGA ACT GAT TAC AAA CAT TGG CCG CAA ATT GCA
	N2-Reverse RPA primer	TGC TTA TTC AGC AAA ATG ACT TGA TCT TTG AAA
	N2-Forward Cas12a gRNA	UAA UUU CUA CUA AGU GUA GAU AAC GCU GAA GCG CUG GGG GC
	N2-Reverse Cas12a gRNA	UAA UUU CUA CUA AGU GUA GAU GGU UGA CCU ACA CAG GUG CC
	RPP30-Forward RPA primer	TAT GCG GCC TCG GAC TTC AGC ATG GCG GTG
	RPP30-Reverse RPA primer	ATC CCA GAG ACT CTG GGA GAC CGC AAC TCA C
	RPP30-Forward Cas12a gRNA	UAA UUU CUA CUA AGU GUA GAU CUC GCA GGU CCA AAU CUG CA
	RPP30-Reverse Cas12a gRNA	UAA UUU CUA CUA AGU GUA GAU UUG UGG AGA CAG CCG CUC AC
	Reporter probe (5 mer)	FAM–TTA TT
	Reporter probe (7 mer)	FAM–TAT TAT T
	Reporter probe (9 mer)	FAM–TAT TAT TAT
	Reporter probe (11 mer)	FAM–ATT ATT ATT AT
	Reporter probe (13 mer)	FAM–ATT ATT ATT ATT A
SARS-CoV-2 N1 for IVT[b]	Forward primer	TAA TAC GAC TCA CTA TAG GGC TCA AGG AAC AAC ATT GCC A
	Reverse primer	GCT TTA GTG GCA GTA CGT T
SARS-CoV-2 N1 for qRT-PCR	Forward primer	CAG CAG TAG GGG AAC TTC T
	Reverse primer	AGA CAT TTT GCT CTC AAG CTG

[a] The colors of oligonucleotide sequences correspond to those of the domains depicted in Fig. 1(a).
[b] Underlined sequence is a T7 promoter sequence.

Table S2. Information of clinical samples.

Patient #	Age	Gender	COVID-19	Patient #	Age	Gender	COVID-19
1	62	Male	Positive	**11**	41	Female	Negative
2	62	Female	Positive	**12**	37	Female	Negative
3	69	Female	Positive	**13**	80	Female	Negative
4	60	Male	Positive	**14**	34	Female	Negative
5	60	Male	Positive	**15**	18	Male	Negative
6	62	Male	Positive	**16**	34	Female	Negative
7	50	Male	Positive	**17**	14	Female	Negative
8	79	Female	Positive	**18**	40	Female	Negative
9	64	Female	Positive	**19**	25	Female	Negative
10	23	Male	Positive	**20**	21	Male	Negative

Table S3. Comparison of COVID-19 molecular tests.

System	Readout	Assay time (min)	LOD (copy/μL)	Assay characteristics	Reference
Dual-functional plasmonic system	LSPR	14	1.13×10^5	• Specialized chip from microfabrication • Low sensitivity	1
Sandwich electrochemical sensor	Electrochemistry	180	0.2	• Many assay steps including magnetic separation • Long assay time	2
RT-PCR	Fluorescence	120	3.2	• Requiring precise temperature control • Dual-labeled probe (fluorophore and quencher) • Long assay time	3
RT-LAMP	Color	20	0.5	• Complex primer design • Isothermal amplification	4
RT-RPA	Fluorescence	20	1.2	• Dual-labeled probe • Isothermal amplification • 2 steps	5
NEAR	Fluorescence	17	20	• Dual-labeled probe • Isothermal amplification	6
NASBA	Fluorescence	120	2.5	• Long assay time • Isothermal amplification • 2 steps	7
RT-LAMP & CRISPR/Cas	Color	40	10	• Complex primer design • Isothermal amplification • 2 steps	8
RT-RPA & CRISPR/Cas	Fluorescence	50	0.07	• Dual-labeled probe • Isothermal amplification • 2 steps	9
CODA (current work)	Fluorescence anisotropy	20	3	• Isothermal amplification • Ratiometric measurements • Single step	-

References

1. Qiu, G. et al. Dual-functional plasmic photothermal biosensors for highly accurate severe acute respiratory syndrome coronavirus 2 detection. *ACS Nano* **14**, 5268-5277 (2020).
2. Zhao, H. et al. Ultrasensitive supersandwich-type electrochemical sensor for SARS-CoV-2 from the infected COVID-19 patients using a smartphone. *Sens Actuators B: Chem* **327**, 128899 (2021).
3. Lu, X. et al. US CDC Real-Time Reverse Transcription PCR Panel for Detection of Severe Acute Respiratory Syndrome Coronavirus 2. *Emerg Infect Dis* **26**, (2020).
4. Yu, L. et al. Rapid Detection of COVID-19 Coronavirus Using a Reverse Transcriptional Loop-Mediated Isothermal Amplification (RT-LAMP) Diagnostic Platform. *Clin Chem* **66**, 975-977 (2020).
5. Behrmann, O. et al. Rapid Detection of SARS-CoV-2 by Low Volume Real-Time Single Tube Reverse Transcription Recombinase Polymerase Amplification Using an Exo Probe with an Internally Linked Quencher (Exo-IQ). *Clin Chem* **66**, 1047-1054 (2020).
6. Zhen, W., Smith, E., Manji, R., Schron, D. & Berry, G. J. Clinical Evaluation of Three Sample-to-Answer Platforms for Detection of SARS-CoV-2. *J Clin Microbiol* **58**, (2020).
7. Wu, Q. et al. INSIGHT: a population scale COVID-19 testing strategy combining point-of-care diagnosis with centralised high-throughput sequencing. (2020).
8. Broughton, J. P. et al. CRISPR-Cas12-based detection of SARS-CoV-2. *Nat Biotechnol* **38**, 870-874 (2020).
9. Huang, Z. et al. Ultra-sensitive and high-throughput CRISPR-powered COVID-19 diagnosis. *Biosens Bioelectron* **164**, 112316 (2020).